

HIGH-RESOLUTION IMAGING OF ORDERED MIXED-LAYER CLAYS

ROBERT E. KLIMENTIDIS

Exxon Production Research Company, P.O. Box 2189, Houston, Texas 77001

IAN D. R. MACKINNON¹

Microbeam Inc., P.O. Box 590267, Houston, Texas 77259

Abstract—High-resolution transmission electron microscopy (HRTEM) has been used to examine illite/smectite from the Mancos Shale; rectorite from Garland County, Arkansas; illite from Silver Hill, Montana; Na-smectite from Crook County, Wyoming; corrensite from Packwood, Washington; and diagenetic chlorite from the Tuscaloosa Formation. Thin specimens were prepared by ion milling, ultramicrotome sectioning, and/or grain dispersal on a holey carbon substrate. Some smectite-bearing clays were also examined after intercalation with dodecylamine hydrochloride (DH). Intercalation of smectite with DH proved to be a reliable method for HRTEM imaging of expanded smectite ($d(001) = 16 \text{ \AA}$) which could then be distinguished from unexpanded illite ($d(001) = 10 \text{ \AA}$). Lattice fringes of basal spacings of DH-intercalated rectorite and illite/smectite showed a 26-\AA periodicity. These data support X-ray powder diffraction (XRD) studies which suggest that these samples are ordered, interstratified varieties of illite and smectite. The ion-thinned, unexpanded corrensite sample showed discrete crystallites containing 10-\AA and 14-\AA basal spacings corresponding to collapsed smectite and chlorite, respectively. Regions containing disordered layers of chlorite and smectite were also noted. Crystallites containing regular alternations of smectite and chlorite layers were not common. These HRTEM observations of corrensite did not corroborate XRD data. Particle sizes parallel to the c axis ranged widely for each sample studied, and many particles showed basal dimensions equivalent to more than five layers. For all illite, smectite, and illite/smectite particles examined, crystallite sizes of about 20 \AA in the basal dimension were not observed.

Key Words—Chlorite, Corrensite, High-resolution transmission electron microscopy, Illite, Lattice imaging, Mixed layer, Particle size, Rectorite, Smectite.

INTRODUCTION

Until recently, X-ray powder diffraction (XRD) has been the major technique used to understand the structural arrangements of mixed-layer clay minerals. Even though XRD allows precise, routine measurements of atomic spacings, values derived are averaged over extremely large volumes relative to atomic spacings. In contrast, selected-area electron diffraction (SAD), conventional transmission electron microscopy (TEM), and high-resolution transmission electron microscopy (HRTEM) sample smaller regions (e.g., $\sim 1000 \text{ \AA}$ for SAD and $< 5 \text{ \AA}$ for phase-contrast imaging) and can provide complementary data on the particle sizes, unit-cell dimensions, and localized atomic arrangements of individual clay grains.

In recent years, acquisition of structural and chemical data from specimen areas as small as 200 \AA in diameter has become possible with the development of HRTEM coupled with energy-dispersive X-ray spectroscopy (EDX) for elemental analysis. Under ideal conditions, image resolution of about 3 \AA (point-to-point) can be routinely obtained on mineral specimens.

The combined structural and chemical capability of the analytical electron microscope (AEM) represents a powerful new tool for the investigation of complex, fine-grained minerals such as mixed-layer clays.

Mixed-layer clays are abundant in sedimentary rocks and are considered important indicators of diagenetic alteration (Hower *et al.*, 1976; Hower, 1981a, 1981b). The most common and well-studied mixed-layer clay minerals are members of the illite/smectite (I/S) group. Numerous studies on the identification, kinetics, and synthesis of I/S can be found in the literature (e.g., Eberl and Hower, 1976; Eberl, 1978; Roberson and Lahann, 1981; Garrels, 1984); however, the mechanism of the smectite-to-illite transition during burial is not well understood.

Models of layer arrangements in mixed-layer clays have been developed based on XRD and Monte Carlo numerical simulation studies. Models based on XRD data were extensively illustrated by Reynolds and Hower (1970), Reynolds (1967), and Brindley and Brown (1980). Recently, Bethke and Altaner (1986) modeled the formation of I/S clays based on a Monte Carlo numerical simulation using a nearest-neighbor illitization scheme. Their work, which adequately explained XRD patterns for many naturally occurring I/S clays, suggests that the I/S transformation mech-

¹ Present address: Department of Geology, University of New Mexico, Albuquerque, New Mexico 87131.

Table 1. X-ray powder diffraction data for oriented sample mounts of reference clays.

Smectite (SWy-1) ¹		Illite (IMt-1) ²	Illite/smectite (ISMt-1) ³		Rectorite (RAR-1) ⁴		Corrensite (CorWa-1) ⁵				
Air dried <2 μm (Mg-sat) ⁷ d (Å)	DH ⁶ <2 μm (Mg-sat) d (Å)		Air dried <0.2 μm d (Å)	Ethylene glycol <0.2 μm (Mg-sat) d (Å)	Air dried <0.2 μm (Na-sat) d (Å)	Ethylene glycol <2 μm (Mg-sat) d (Å)	Air dried <2 μm (Mg-sat) d (Å)	Glycerol <2 μm (Mg-sat) d (Å)	Ethylene glycol <2 μm (Mg-sat) d (Å)	550°C <2 μm (Mg-sat) d (Å)	DH ⁶ <2 μm d (Å)
14.98	16.51	10.16	12.08	31.0	22.6	27.67	29.1	31.5	29.45	23.9	29.45
8.51	8.71	7.24	9.21	14.09	11.2	13.56	14.5	15.8	14.25	12.3	15.24
5.54	5.90	5.45	7.27	9.51	7.25	10.13	9.61	14.4	9.31	7.8	7.79
4.77	4.44	5.03	5.08	5.30	5.50	9.01	7.14	8.04	7.08		
3.32	3.32	4.52	4.52	4.52	4.90	7.24	5.27	7.3			
2.88		3.36	4.30	4.31	4.46	6.72	4.77	4.62			
			3.37	3.36	4.16	6.29	3.56				
			3.24	2.30	3.56	5.37	3.21				
			2.90	2.22	3.34	5.03	2.85				

¹ SWy-1. Na-Montmorillonite, Crook County, Wyoming.

² IMt-1. Illite, Silver Hill, Montana (Cambrian shale).

³ ISMt-1. Illite/smectite, Mancos Shale (Ordovician).

⁴ RAR-1. Rectorite, Garland County, Arkansas.

⁵ CorWa-1. Corrensite, Packwood, Washington (Eocene).

All above samples are from the Source Clay Repository offered by The Clay Minerals Society.

⁶ DH = dodecylamine hydrochloride.

⁷ Mg-sat = Mg-saturated mount.

anism involves a number of individual rate laws or reaction steps which may vary throughout the illitization process. Sub-unit-cell imaging in real space using HRTEM can provide the necessary experimental control for both types of mixed-layer modeling procedures. The present paper reports an AEM study of well-known mixed-layer clays combined with complementary XRD in order to provide a basis for verification of current mixed-layer stacking models and/or a more detailed understanding of mixed-layer clay formation.

EXPERIMENTAL

Samples

Individual samples of illite, smectite, chlorite, and ordered mixed-layer clays, such as illite/smectite (rectorite) and chlorite/smectite (corrensite), were selected for study. All samples, except the chlorite from the Tuscaloosa Formation, are from the Source Clays Repository of The Clay Minerals Society. A compilation of XRD data collected on specimens used in this study is given in Table 1.

Sample SWy-1 is a sodium smectite from the Cretaceous Newcastle bentonite formation, Crook County, Wyoming. Characterization data for this smectite were summarized by van Olphen and Fripiat (1979). Our XRD data for sample SWy-1 revealed a $d(001)$ value of 14.98 Å for the air-dried, Mg-saturated material which expanded to 16.51 Å upon intercalation with dodecylamine hydrochloride (DH). This value agrees reasonably well with the $d(001)$ value of 15.67 Å reported by Ruehlicke and Kohler (1981) for the DH-intercalate of this smectite.

Sample IMt-1 is an illite from a Cambrian shale in the Silver Hill Formation, Jefferson Canyon, Montana, and was described as a 1Md polytype by Hower and Mowatt (1966). XRD revealed at 10-Å basal spacing in air. Intercalation with DH caused no expansion of the basal spacing.

Sample ISMt-1 is a mixed-layer I/S and is the primary clay type in the Cretaceous Mancos Shale in Montana (Nadeau and Reynolds, 1981). Our interpretation of XRD data using the methods of Reynolds (1967) and Reynolds and Hower (1970) and subsequent modifications by Środoń (1980, 1981, 1984) indicates that the sample is an ordered (R=1) I/S with about 80% illite layers.

Sample RAR-1, a rectorite from Garland County, Arkansas, was described by Miser and Milton (1964). Our comparison of XRD data for this sample with those reported by Reynolds and Hower (1970) indicates that this mineral is a regularly interstratified I/S with R=1 ordering and 50% illite layers. Środoń's (1980) data also indicate about 50% illite layers. The XRD pattern of the sample heated at 550°C showed a reflection at 9.93 Å, which corresponds to the spacing of collapsed smectite layers. Minor amounts of discrete illite and koalinite were also detected.

Corrensite sample CorWa-1 is from the Ohanapcosh Formation, an altered late-Eocene tuff, in Packwood, Washington. This sample satisfies the diagnostic XRD criteria for an ordered chlorite/smectite (Brindley and Brown, 1980), including a Mg-saturated $d(001)$ value of 30.4 Å, which expands to about 32.7 Å with glycerol solvation and collapses to 23.8 Å on heating to 500°C (David R. Pevear, Exxon Production Research Company, Houston, Texas, and Phoebe L. Hauff,

The Clayschool, Conifer, Colorado, personal communication, 1985). Minor amounts of discrete chlorite were detected in the XRD trace of the Mg-saturated, glycerol-solvated sample (peaks at 14.4 and 7.3 Å).

The chlorite specimen used in this study is from the late Cretaceous Tuscaloosa Formation, Louisiana. Electron microprobe analyses showed it to be Fe-rich and to contain about 33% FeO and 6% MgO. XRD gave typical basal reflections for pure chlorite: $d(001) = 14.0$ Å, $d(002) = 7.03$ Å, and $d(003) = 3.52$ Å. HRTEM images showed typical two-dimensional structure such as observed by Spinnler *et al.* (1984) on a clinocllore chlorite from West Chester, Pennsylvania.

Sample preparation

Three standard specimen preparation techniques were used: ion-beam thinning, ultramicrotomy, and particle dispersion. For bulk samples, where material availability or purity was not a concern (e.g., samples ISMt-1 and IMt-1), ultrathin sections were prepared by ion milling (Barber, 1970; Phakey *et al.*, 1972; Paulus *et al.*, 1975) 3-mm diameter regions after they were removed from petrographic thin sections of standard thickness (30 µm). This method allowed correlation between optical thin-section petrography, scanning electron microscopy (SEM), and HRTEM. In addition, this approach preserved the natural assemblage of all constituents of a sediment and readily provided important microtextural data (e.g., grain shape and size).

Clay powders of size-fractionated clays (e.g., <0.2 µm) from a bulk specimen were particularly difficult to image along the *c* axis. In some samples, particles dispersed on a holey carbon substrate were imaged along *c* at the particle edges, if these edges curled or were fortuitously oriented. Aspects of this technique, including limitations of HRTEM interpretation, were described by McKee and Brown (1977). For the present study, only smectites produced well-oriented *c* axes at the edges of particles (see Figures 2a and 2b). An alternative preparation of clay powders involved epoxy embedding and ultramicrotomy. An oriented clay-layer mount was obtained by air drying droplets of a sample suspension between beds of cured epoxy (Spurr, 1969). The resulting cured epoxy-clay sandwich was then sectioned perpendicular to the basal direction following the procedures outlined by Eberhart and Triki (1972), Tchoubar *et al.* (1973), and Brown and Jackson (1973).

As shown in Figure 2a, and implied in a previous HRTEM study by Kohyama *et al.* (1982), smectitic clays may collapse under vacuum. This phenomenon precludes reliable interpretation of untreated I/S clays, inasmuch as illite layers and collapsed smectite layers may be dimensionally similar in a HRTEM image. To overcome this problem, samples SWy-1, ISMt-1, and RAr-1 were intercalated with DH using a simplified

version of the procedure outlined by Ruehlicke and Kohler (1981).

Lagaly and Weiss (1969) used XRD to show that for small inorganic ions in the interlayer site (Na^+ , Mg^{2+} , Ca^{2+}), the basal spacings of dried, DH-intercalated clays are not markedly influenced by changes in the layer charge. Expansion of the intercalated clay persists for a few months at atmospheric pressure (Lagaly and Weiss, 1969) and also for several weeks in the AEM sample chamber. Upon intercalation with DH, the basal spacings for <2-µm size, Mg^{2+} -saturated smectite SWy-1 expanded from 14.98 to 16.51 Å (see Table 1). This basal expansion of sample SWy-1 with DH intercalation was also confirmed by HRTEM imaging. Both XRD and HRTEM imaging of DH-treated illite (sample IMt-1) showed no expansion of the basal spacing.

An alternative method in which low-viscosity epoxy (Spurr, 1969) is used to expand smectites (Tessier and Pedro, 1982) was also investigated for sample SWy-1. Preliminary data suggest that smectite layers consistently expanded to 15 Å.

Microscopy

All samples were studied at an accelerating voltage of 200 kV. Selected samples were also analyzed at 100, 120, 300, and 400 kV. The transmission electron microscopes used for this study were side-entry goniometer versions of the JEOL 100CX, Philips EM 420T, JEOL 200CX, JEOL 2000FX, Philips EM300T, and JEOL 4000EX instruments. Some of the variation in quality of the data presented in Figures 1–5 is related to both imaging resolution and operating voltage, as well as to the nature of the specimen (i.e., rate of electron beam damage) and the preparation technique. Nevertheless, basal spacings of the clays were readily observed and were interpretable in all images. Measurements of lattice fringes were calibrated for each microscope using standard imaging specimens (usually graphitized carbon, where $d(002) = 3.4$ Å or beryl, where $d(001) = 9.2$ Å) and by calibrating the appropriate SAD patterns using a thin Au coating on each sample for each particular operating condition. The error in lattice image measurements and SAD patterns was estimated to be ±2% relative. In some experiments, relative lattice fringe spacings were confirmed by calibrated optical scans of the TEM negative using a Joyce Loebel Model 3CS microdensitometer.

In all experiments, the basal spacing of interest was considerably greater than the nominal point-to-point resolution of any microscope used. Our interpretation of these HRTEM images was restricted to measurements of basal spacings and, where possible, cross-fringes if a crystallite was appropriately oriented. Inasmuch as optimal imaging conditions were not always possible, a relatively stable sample of chlorite (Tuscaloosa Formation) was used to confirm general im-

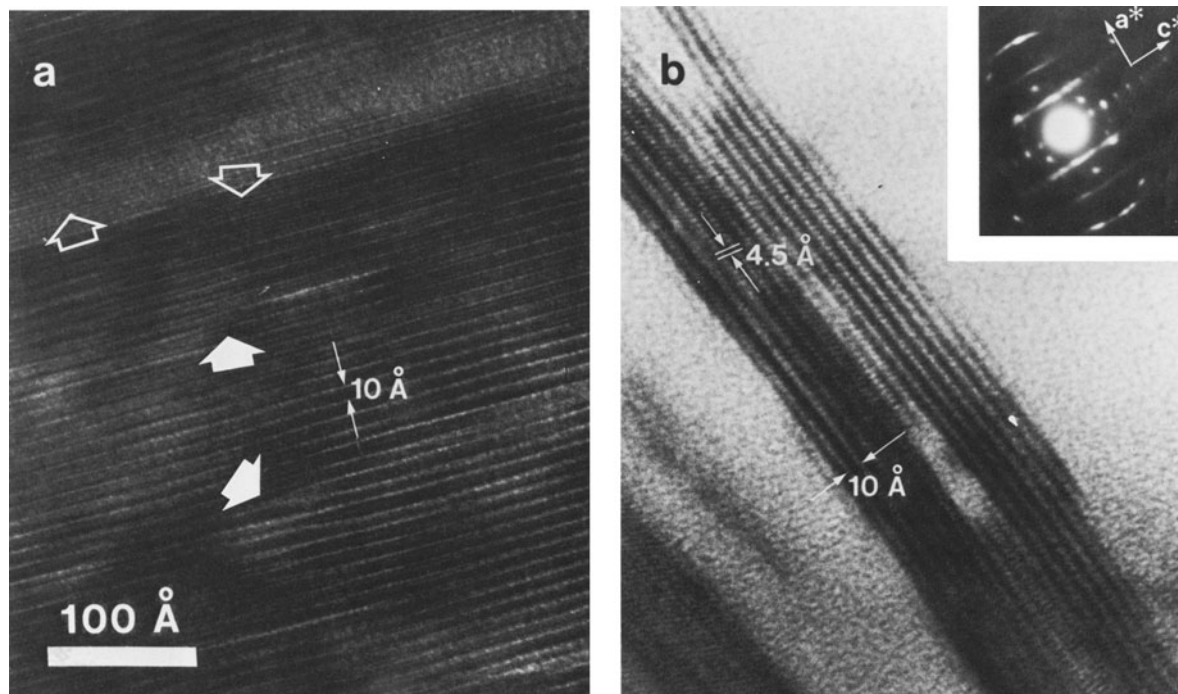


Figure 1. High-resolution lattice images of illite (IMt-1) from an ion-thinned section: (a) lattice fringes showing typical 10-Å spacing. Note layer termination and “pinch and swell” (solid arrows) in this relatively large (~30 layers) crystallite; sublattice fringes of ~5 Å occur where imaging conditions are favorable (open arrows); (b) two-dimensional image of well-oriented crystallites (~10 layers) showing 10- and 4.5-Å lattice fringes; selected area electron diffraction pattern (insert) shows intense streaking in higher order reflections suggesting layer-stacking disorder.

aging principles (Spence, 1981) for lattice fringes from layer silicates. Many of these principles have been supported by extensive model calculations on silicates (Iijima and Buseck, 1978; O’Keefe *et al.*, 1978; Spinnler *et al.*, 1984). For example, O’Keefe *et al.* (1978) showed that fringe contrast reversal can be observed over a relatively large range of defocus for silicate minerals. This particular feature was verified in the present study using the Tuscaloosa chlorite. Although the detailed relationship of image contrast to the atomic structure is not known with certainty, the 14-Å basal repeat distance (calibrated with SAD patterns) remained constant throughout this optimum defocus range.

The understanding that an array of lattice fringes shows the minimum particle dimension (or crystallite size) normal to the direction of the fringes is implicit in all interpretations in this paper. This dimension is a minimum value because a particular crystallite or particle may bend or curve away from the electron optic axis. Under such circumstances, lattice fringes would not necessarily be apparent. This aspect of lattice imaging is germane to randomly oriented clay particles such as the ion-milled specimens shown in Figures 1, 3a, and 5. This characteristic of basal lattice fringes is a fundamental advantage offered by HRTEM imaging and can be used even when particle sizes are too small

to provide reliable SAD data (see e.g., Mackinnon and Buseck, 1979).

The rapid rate of electron beam damage for all clays (except the Tuscaloosa chlorite) precluded optimal orientation of specimens using conventional tilting methods. Perfect orientation for basal spacings was assumed if two-dimensional structure images were obtained (i.e., ~4.5-Å cross-fringes, corresponding to $d(020)$) or if basal spacings were observed through a large range of defocus (~1000 Å). These observations were supported by SAD patterns where possible. In general, the rate of electron beam damage decreased with increased operating voltage. Beam damage also decreased for individual clay specimens in the order: smectite, illite, illite/smectite, chlorite/smectite, chlorite. The rate of beam damage decreased by about a factor of 2 between 200 and 400 kV accelerating voltages. Further details of HRTEM imaging were given by Spence (1981) and Eberhart (1981).

OBSERVATIONS

A range of textures and slightly different orientations of the basal plane in two ion-thinned sections of illite IMt-1 are shown in Figures 1a and 1b. In Figure 1a, the c axis for most of the crystallite was normal to the electron optic axis, and, thus, lattice fringes corresponding to 10-Å basal repeats were produced. For this

particular microscope (JEOL 2000FX), sub-unit-cell periodicity ($\sim 5 \text{ \AA}$) was also observed in suitable parts of the crystal (open arrows, Figure 1a). Figure 1b is also an HRTEM image of the illite c axis perpendicular to the electron optic axis, as shown by the SAD pattern of this general region of the section (insert, Figure 1b). This orientation and phase-contrast imaging gave a two-dimensional structure image of the crystallite. Thus, relatively well-ordered, 10-\AA periodicity was observed. Stacking disorder in a^* , however, is also shown in the SAD pattern and the HRTEM image (Figure 1b). Figures 1a and 1b indicate that crystallites of sample IMt-1 contain periodicity in more than one dimension (i.e., directions normal to c) and that no 20-\AA , "fundamental" illite crystals were present in this sample. The crystallite size (i.e., the number of coherently diffracting lattice planes) ranged from 70 to 500 \AA for this illite.

Dispersed particle mounts of smectite SWy-1 were examined before and after intercalation with DH. Figure 2a is a HRTEM image of a particle without DH intercalation. The characteristic 10-\AA basal repeat for collapsed smectite can be seen at the edge of the particle where imaging conditions were favorable. The rapid rate of electron beam damage and the predominant particle orientation made it difficult to image many grains with basal spacings or to estimate the average particle size in this sample; however, Figure 2a indicates that some particles of sample SWy-1 are at least a few layers thick. Isolated examples of particles intercalated with DH showed an expanded basal spacing of 16 \AA , in accord with the XRD data. Figure 2b shows lattice fringes of particles of sample SWy-1 intercalated with DH and then impregnated with Spurr epoxy prior to sectioning with an ultramicrotome. Particle size in the basal direction ($\sim 150 \text{ \AA}$), as well as expansion of the smectite lattice to 15 \AA , is apparent.

A HRTEM image of an ion-thinned sample of ISMt-1, an interstratified I/S containing 80% illite layers, is shown in Figure 3a. This image, obtained at an operating voltage of 400 kV, exhibits considerable detail within the 10-\AA basal spacings. Regions in Figure 3a without lattice (or structure) images may be areas in which the clay was not well oriented, i.e., where zone axes were not parallel to the electron optic axis. Inasmuch as this sample was prepared without intercalation or epoxy embedding, basal spacings for illite and collapsed smectite could not be distinguished. Nevertheless, the crystallite size shown is typical for this sample (whether I/S or discrete smectite and/or illite) and is as large as 90 \AA in the basal direction.

Figure 3b shows basal spacings of dispersed particles of sample ISMt-1 after intercalation with DH. A relatively large region of the field of view shows a consistent 26-\AA basal spacing. Moreover, because this sample was sufficiently stable in the electron beam we were able to obtain a SAD pattern (insert; Figure 3b), where the 26-\AA basal spacing reflections were con-

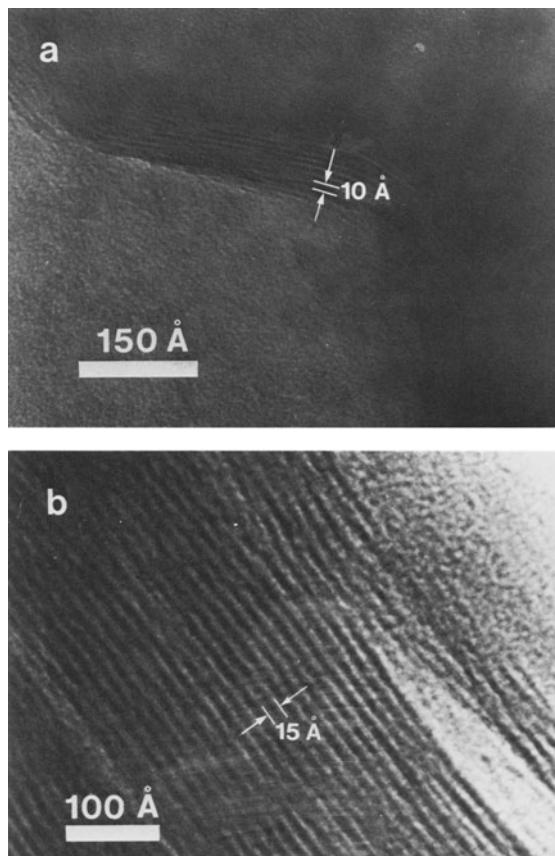


Figure 2. High-resolution lattice images of smectite (SWy-1): (a) prepared as dispersed particles, showing collapsed 10-\AA basal spacings at curled edge of grain; (b) prepared by embedding and ultramicrotomy; note greater number of (expanded) basal spacings and consistency of expansion for each layer; crystallite size is > 15 layers in c axis direction.

firmed. Therefore, the HRTEM image and SAD pattern are due to an ordered arrangement of illite (10 \AA) and expanded smectite (16 \AA) layers. Sub-lattice fringes (e.g., 10 \AA and/or 16 \AA) were not observed because imaging conditions such as orientation and defocus could not be optimized for this sample. Nevertheless, the basal spacing could be measured, and this sample shows a regular arrangement of 8 mixed layers. Figure 3 shows an example of a clay similar to that studied by Nadeau *et al.* (1984a, 1984b); however "fundamental" 20-\AA (illite) particles are not present. XRD data (Table 1) confirmed that sample ISMt-1 is an ordered ($R=1$) I/S clay. Discrete illite particles were not recognized in this sample, perhaps due to a small tendency for grain edges to curl or roll as in smectite and halloysite (McKee *et al.*, 1973).

Images from two dispersed samples of rectorite (RAR-1) are shown in Figure 4. In untreated sample RAR-1, 10-\AA basal spacings from the edges of a dispersed grain were common (Figure 4a). Upon intercalating the sample with DH, a range of basal spacings

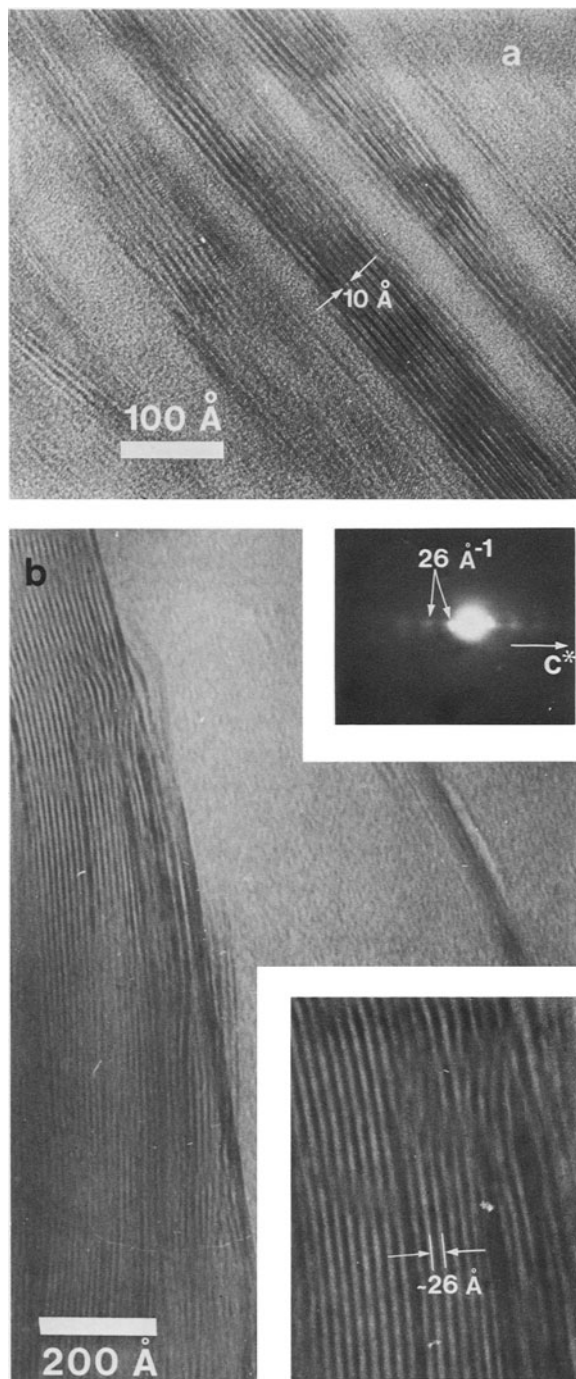


Figure 3. High-resolution lattice images of illite/smectite (ISMt-1): (a) ion-thinned sample showing consistent 10-Å basal spacing which corresponds to either illite or collapsed smectite; each crystallite is ~ 9 layers thick along c axis with sub-parallel orientation; (b) dispersed particle intercalated with dodecylamine hydrochloride showing extensive regions (~ 10 layers) of expanded 26-Å basal spacings; SAD pattern (insert, top) also shows weak 26-Å spacing, corresponding to regularly alternating layers of illite and expanded smectite.

from 26 to 40 Å were observed in dispersed grains (Figure 4b). Spacings of 26 Å were the most common, and, here also, these basal spacings are likely due to a regular arrangement of illite and expanded smectite layers. Larger basal spacings in this sample may have been due to variations in layer charge (Yoshida and Suito, 1972). As with sample ISMt-1, the XRD data for sample RAr-1 indicate that the sample is an ordered ($R=1$), mixed-layer I/S clay.

Corrensite CorWa-1 was considered by David R. Pevear (Exxon Production Research Company, Houston, Texas) and Phoebe Hauff (The Clayschool, Conifer, Colorado, personal communication) to be a well-ordered chlorite/smectite (C/S). Thus, HRTEM images along the c axis direction of crystallites in untreated sample CorWa-1 should have shown basal spacings of 14 and 10 Å, corresponding to chlorite and collapsed smectite, respectively. Figure 5 shows the four predominant types of basal spacings observed in this corrensite. Most crystallites contained only 10- or 14-Å basal spacings. Figure 5a is a typical example of chlorite and shows 14-Å fringes throughout a single crystallite. Identification of this grain as a chlorite has been confirmed with SAD and thin-film EDX analyses. Other commonly observed crystallites show regular arrangements of 14-Å basal spacings with randomly interspersed 10-Å spacings (Figure 5b). A few reverse arrangements of 14-Å fringes interspersed among predominantly 10-Å basal spacings were also noted. Figure 5c shows two adjacent crystallites no more than 10 layers wide in which the basal spacings of 10 and 14 Å are perpendicular to the electron optic axis. The image contrast and fine-scale variations in the 10-Å basal spacings of the collapsed smectite indicate a higher degree of structural disorder compared with the adjacent chlorite crystallite. Crystallite sizes for a variety of C/S layer arrangements ranged from 98 to 210 Å.

A few uncommon examples of regular mixed-layer C/S are shown in the HRTEM images in Figure 5d. Here, approximately two layers of the crystallite show a consistent 24-Å basal spacing which are probably regular alternations of 10- and 14-Å layer spacings. This layer stacking is an excellent example of a regularly alternating ordered C/S clay, but basal spacings of particles on either side of the mixed-layer structure are predominantly 14 Å. Examination of three ion-thinned sections from separate mounts of sample CorWa-1 indicates that arrangements of alternating chlorite and (collapsed) smectite layers are uncommon. These data are not in general agreement with interpretations of XRD data obtained in this study.

DISCUSSION

Interpretation of one- and two-dimensional layer silicate images has been extensively treated in the literature (Iijima and Buseck, 1978; Eggleton and Buseck, 1980; Amouric *et al.*, 1981; Spinnler *et al.*, 1984). These

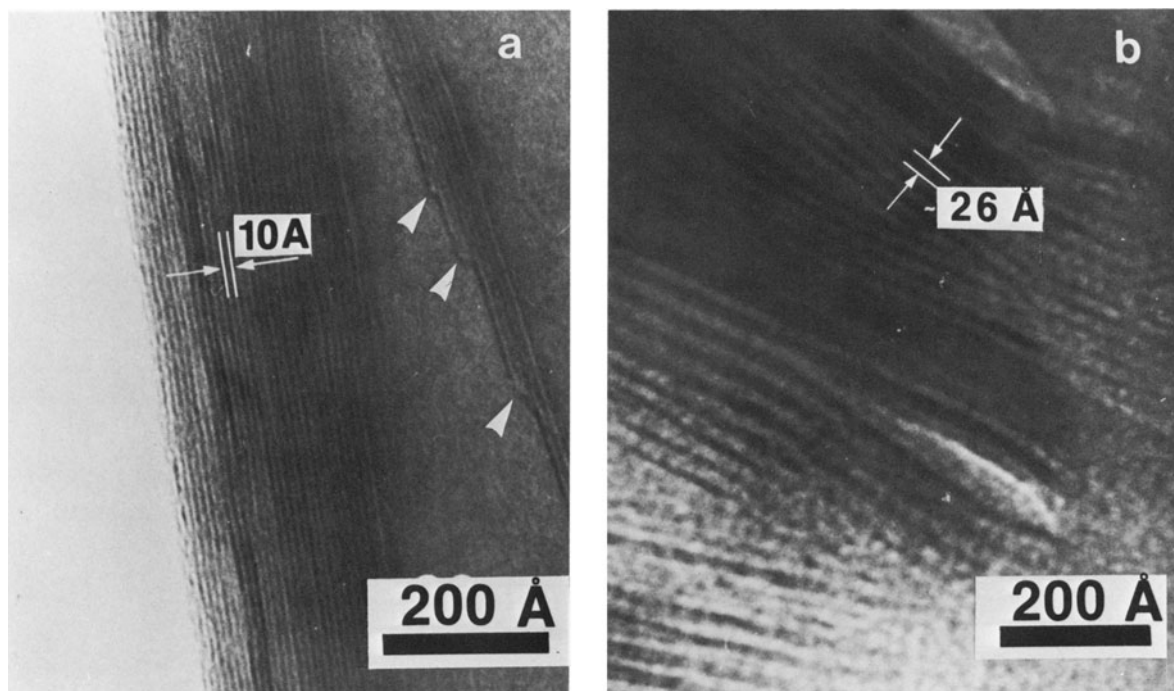


Figure 4. High-resolution lattice images of dispersed particles of rectorite (RAR-1): (a) without intercalation, showing alternating layers of illite and collapsed smectite; (b) after intercalation with dodecylamine hydrochloride, showing regions of expanded 26-Å (and larger) basal spacings; note edge-terminated layer spacings in Figure 4a (arrowed).

studies have shown that experimental and computed image contrast for each set of operating conditions must be compared in order to interpret the details of two-dimensional, sub-unit-cell images. Interpretation of basal spacings and relative interlayer distances is reliable under multiple-beam, bright-field imaging conditions if fringes show optimum contrast (Veblen, 1983). These conditions have been employed for all experiments reported in the present study.

The interpretation of mixed-layer lattice fringes may be ambiguous under certain circumstances, such as in the examination of untreated I/S clays using HRTEM. The ambiguity in interpretation depends, in part, upon the degree of collapse of a smectite layer in the high vacuum of the microscope. Page and Wenk (1979) and Ahn and Peacor (1986) indicated that untreated smectites show a range of basal spacings $>10 \text{ \AA}$, averaging about 13 \AA . Eggleton's (1984) data on an altered olivine and our example in Figure 2a, show that untreated smectites also collapse to a $10\text{-}\text{\AA}$ basal spacing. Collapse of smectite layers may be caused by specimen preparation of ion-thinned samples, as noted by Eggleton (1984), or, as was inferred above for dispersed particles of sample SWy-1, by exposure to a high vacuum during TEM operation. Both expanded and collapsed layers therefore can be found in untreated smectites, but the degree of layer collapse is a highly variable function of specific composition and/or degree of order of each smectite crystal, length of time in vacuum or

under the electron beam, cleanliness and level of vacuum, operating voltage, etc. In addition, disordered I/S may show layer-collapse characteristics quite different from that of discrete smectite or well-ordered I/S (i.e., rectorite). Thus, the presence of a basal spacing $>10 \text{ \AA}$ may not be sufficient to distinguish all smectites from illites within a mixed-layer I/S clay.

Ahn and Peacor (1985) and Lee *et al.* (1985) indicated that illite and untreated smectite may be distinguished by common structural and crystallinity features within specific sedimentary sequences. For example, Ahn and Peacor (1986) suggested that illites in Gulf Coast argillaceous sediments contain lattice fringes which are continuous and straight for greater distances (i.e., larger crystallites) than smectites and that they are relatively defect-free. Although these criteria appear valid for this particular sequence of clays, the illite shown in Figures 1a and 1b include lattice fringes of variable width (>15 layers, Figure 1a; 4 layers, Figure 1b), as well as a number of intralayer defects (arrowed, Figure 1a), layer pinch and swell, and layer terminations. By comparison, the basal spacings for DH-treated smectite (Figure 2b) are relatively continuous and defect-free.

The HRTEM imaging and SAD of I/S clays in this study confirm the conventional interpretation of XRD data for well-ordered ($R=1$) mixed-layer clays. Regular alternations of illite and expanded smectite producing sequences of ISISIS . . . , were observed for crystallite

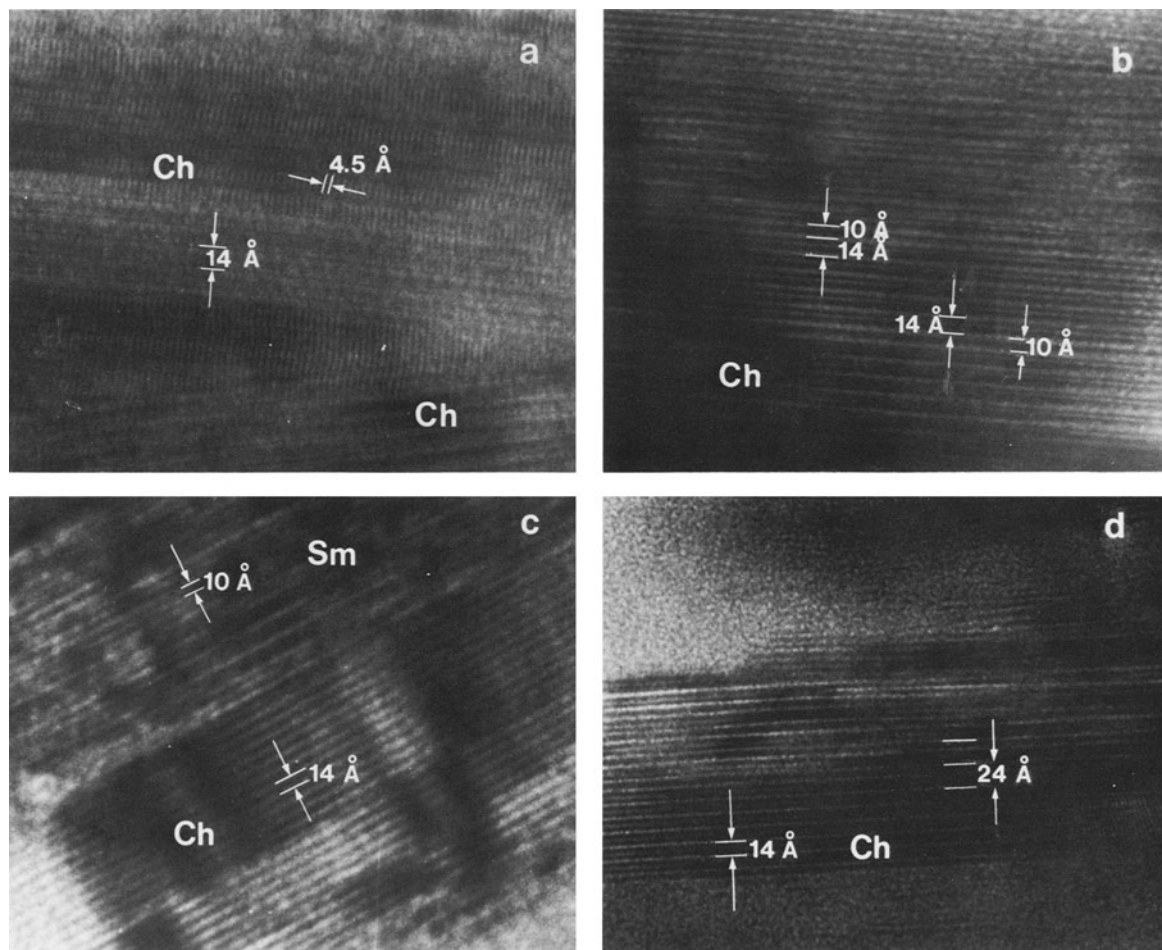


Figure 5. High-resolution lattice images of untreated bulk corrensite showing typical layer arrangements for chlorite (Ch) and collapsed smectite (Sm): (a) large crystals of well-ordered chlorite; (b) smaller crystallites of chlorite with layers of collapsed smectite; (c) chlorite crystallite (~ 10 layers) adjacent to, and oriented with collapsed smectite crystallite; (d) chlorite crystallites adjacent to layers of regularly alternating chlorite and collapsed smectite.

sizes as large as 200 Å along the basal direction in sample ISMt-1. Because of the difficulty in obtaining a representative data set of basal spacings from dispersed particles, we were not able to determine whether large crystallites ($N_c > 5$, where N_c is the number of layers in a particle) of well-ordered, expanded, $R=1$ I/S predominate in samples ISMt-1 or RAr-1. Collecting such data requires a more tractable technique of specimen preparation, such as embedding and ultramicrotomy. Expanded layers in both samples were observed, although not always recorded because of experimental difficulties. Images of these expanded layers suggest that ordered mixed-layer structures of illite and smectite do indeed occur. In addition, for all illite, smectite, and I/S samples examined, particle sizes on the order of 20 Å in the basal direction were not observed.

The data from the present study on the corrensite

from Washington are less definitive than those from sample ISMt-1. Extended crystallites ($N_c > 5$) with regularly alternating layers of chlorite and smectite were not observed. Zones of discrete chlorite, discrete collapsed smectite, and randomly interstratified C/S were common in the bulk sample. Difficulties in image interpretation may arise from the possibility that uncollapsed smectite (~ 14 Å) may be abundant and unusually stable. This possibility would make the distinction of chlorite from smectite very difficult on the basis of lattice periodicity alone. Under the experimental conditions used in the present investigation, however, smectite in these corrensite samples should have collapsed to 10 Å, a spacing commonly observed. Nevertheless, the proportion of discrete chlorite and (collapsed) smectite, as well as randomly interstratified chlorite and smectite, noted by HRTEM was considerably higher than was indicated by bulk XRD analysis.

We cannot fully reconcile the apparent discrepancy between XRD and HRTEM results obtained on sample CorWa-1.

Our observations and those of Yoshida (1973) and McKee and Buseck (1978) do not completely agree with recent TEM studies of a regular I/S (52% illite layers) with R=1 ordering reported by Nadeau *et al.* (1984a, 1984b). Nadeau *et al.* (1984a) estimated that 79% of the particles are only 20 Å thick along the *c* axis direction. In addition, they suggested that this regular I/S consisted of elementary "illite" particles whose interfaces are capable of forming complexes with water and organic molecules. Nadeau *et al.* (1984a, 1984b) argued that these complexes, and thin, parallel particles of illite, showed interparticle diffraction effects which produced XRD patterns similar to those of mixed-layer clays. We have shown here that ordered I/S clays may have particle thicknesses >50 Å, and that regular alternations of illite and expanded smectite layers do indeed occur in some crystals. The basic observations from this study and those of Nadeau *et al.* (1984a, 1984b) provide complementary data on the nature of mixed-layer clay structures.

Two important differences in these studies are apparent in sample preparation and data interpretation. Nadeau *et al.* (1984a, 1984b) used an indirect, less accurate basal spacing determination on a statistically significant data set, whereas our study was based upon fewer significant observations but used a more precise direct-layer measurement technique. Both experimental approaches have merit, and the data on corrensite indicate that interpretations of clay structures may be difficult even when well-ordered interstratification is present.

Finally, XRD profiles derived from a variety of calculated Monte Carlo sequences of illite, smectite, and I/S layers agree well with published XRD patterns from natural samples (Bethke and Altaner, 1986). The Monte Carlo layer sequences (which are based upon an assumed "illitization" mechanism) tend to develop clusters of segregated illite and/or smectite layers, as well as mixed-layer structures. This theoretical description of illite/smectite layer sequences agrees well with experimentally observed layer sequences in some illite/smectite (Lee *et al.*, 1985; Ahn and Peacor, 1985, 1986) and corrensite (sample CorWa-1, this study). Direct calibration of these theoretical studies with both HRTEM and XRD data may provide an accurate description of the mechanism of the illitization reaction for smectite in major sedimentary environments.

ACKNOWLEDGMENTS

We acknowledge fruitful discussions on clay mineralogy with David R. Pevear, Craig S. Calvert, Phoebe L. Hauff, and Tom R. McKee. Encouragement for this study from Mike G. Lafon, Robert H. McCallister, and Theresa F. Schwarzer is appreciated. We also gratefully

acknowledge critical reviews by F. A. Mumpton, P. H. Nadeau, C. M. Bethke, and an anonymous reviewer. Thanks are due to J. H. Lee and D. R. Peacor for providing manuscripts of their work prior to publication. Technical support from Mark S. Shemet, Daniel I. Jezek, and Timothy R. Klett is also greatly appreciated.

REFERENCES

- Ahn, J. H. and Peacor, D. R. (1985) Transmission electron microscopic study of diagenetic chlorite in Gulf Coast argillaceous sediments: *Clays & Clay Minerals* **33**, 228–236.
- Ahn, J. H. and Peacor, D. R. (1986) Transmission and analytical electron microscopy of the smectite-to-illite transition: *Clays & Clay Minerals* **34**, 165–179.
- Amouric, M., Mercuriot, G., and Baronnet, A. (1981) On computed and observed HRTEM images of perfect mica polytypes: *Bull. Mineral.* **104**, 298–313.
- Barber, D. J. (1970) Thin foils of non-metals made for electron microscopy by sputter etching: *J. Mater. Sci.* **5**, 1–8.
- Bethke, C. M. and Altaner, S. P. (1986) A layer-by-layer mechanism of smectite illitization and its application to a new rate law: *Clays & Clay Minerals* **34**, 136–145.
- Brindley, G. W. and Brown G. (1980) *Crystal Structures of Clay Minerals and Their X-ray Identification*: Mineralogical Society Monograph No. 5, Mineralogical Society, London, 495 pp.
- Brown, J. L. and Jackson, M. L. (1973) Chlorite examination by ultramicrotomy and high resolution electron microscopy: *Clays & Clay Minerals* **21**, 1–7.
- Eberhart, J. P. (1981) High resolution electron microscopy applied to clay minerals: in *Advanced Techniques for Clay Mineral Analysis*, J. J. Fripiat, ed., Elsevier, Amsterdam, 31–50.
- Eberhart, S. P. and Triki, R. (1972) Description d'une technique permettant d'obtenir des coupes minces de minéraux argileux par ultramicrotomie. Application à l'étude des minéraux argileux interstratifiés: *J. Microscopie* **15**, 111–120.
- Eberl, D. D. (1978) The reaction of montmorillonite to mixed-layer clay: the effect of interlayer alkali and alkaline earth cations: *Geochim. Cosmochim. Acta* **42**, 1–7.
- Eberl, D. D. and Hower, J. (1976) Kinetics of illite formation: *Geol. Soc. Amer. Bull.* **87**, 1327–1330.
- Eggleton, R. A. (1984) Formation of iddingsite rims on olivine: a transmission electron microscope study: *Clays & Clay Minerals* **32**, 1–11.
- Eggleton, R. A. and Buseck, P. R. (1980) High resolution electron microscopy of feldspar weathering: *Clays & Clay Minerals* **28**, 173–178.
- Garrels, R. M. (1984) Montmorillonite/illite stability diagrams: *Clays & Clay Minerals* **32**, 161–166.
- Hower, J. (1981a) X-ray identification of mixed-layer clay minerals: in *Clays and the Resource Geologist*, F. J. Longstaffe, ed., Mineralogical Association of Canada Short Course Notes, Calgary, Alberta, 39–59.
- Hower, J. (1981b) Shale diagenesis: in *Clays and the Resource Geologist*, F. J. Longstaffe, ed., Mineralogical Association of Canada Short Course Notes, Calgary, Alberta, 60–80.
- Hower, J., Eslinger, E. V., Hower, M. E., and Perry, E. A. (1976) Mechanism of burial metamorphism of argillaceous sediment. 1. Mineralogical and chemical evidence: *Geol. Soc. Amer. Bull.* **87**, 725–737.
- Hower, J. and Mowatt, T. C. (1966) The mineralogy of illites and mixed-layer illite/montmorillonite: *Amer. Mineral.* **51**, 825–854.

- Iijima, S. and Buseck, P. R. (1978) Experimental study of disordered mica structures by high-resolution electron microscopy: *Acta Crystallogr.* **A34**, 709–719.
- Kohyama, N., Fukushima, K., and Fukami, A. (1982) Interlayer hydrates and complexes of clay minerals observed by electron microscopy using an environmental cell: in *Proc. Int. Clay Conf., Bologna, Pavia, 1981*, H. van Olphen and F. Veniate, eds., Elsevier, Amsterdam, 373–384.
- Lagaly, G. and Weiss, A. (1969) Determination of the layer charge in mica-type layer silicates: in *Proc. Int. Clay Conf., Tokyo, 1969, Vol. 1*, L. Heller, ed., Israel Univ. Press, Jerusalem, 61–80.
- Lee, J. H., Ahn, J. H., and Peacor, D. R. (1985) Textures in layered silicates: progressive changes through diagenesis and low temperature metamorphism: *J. Sed. Petrol.* **55**, 532–590.
- Mackinnon, I. D. R. and Buseck, P. R. (1979) New phyllosilicate types in a carbonaceous chondrite matrix: *Nature* **280**, 219–220.
- McKee, T. R. and Brown, J. L. (1977) Preparation of specimens for electron microscopic examination: in *Minerals in Soil Environments*, J. B. Dixon and S. B. Weed, eds., Soil Science Society of America, Madison, Wisconsin, 809–841.
- McKee, T. R. and Buseck, P. R. (1978) HRTEM observations of stacking and ordered interstratification in rectorite: *Proc. 9th Int. Cong. Electron Microsc.* **1**, 272–273.
- McKee, T. R., Dixon, J. B., Whitehouse, M. G., and Harling, D. F. (1973) Study of TePuke halloysite by a high resolution electron microscope: in *Proc. 31st Ann. Meet. Electron Microscopy Soc. Amer.* C. J. Arceneaux, ed., Baton Rouge, Louisiana, 200–201.
- Miser, H. D. and Milton, C. (1964) Quartz, rectorite, and cookeite from the Jeffrey quarry near North Little Rock, Pulaski County, Arkansas: *Arkansas Geolog. Commission Bull.* **21**, 29 pp.
- Nadeau, P. H. and Reynolds, R. C., Jr. (1981) Burial and contact metamorphism in the Mancos Shale: *Clays & Clay Minerals* **29**, 249–259.
- Nadeau, P. H., Tait, J. M., McHardy, W. J., and Wilson, M. J. (1984a) Interstratified XRD characteristics of physical mixtures of elementary clay particles: *Clay Miner.* **19**, 67–76.
- Nadeau, P. H., Wilson, M. J., McHardy, W. J., and Tait, J. M. (1984b) Interstratified clays as fundamental particles: *Science* **225**, 923–925.
- O'Keefe, M. A., Buseck, P. R., and Iijima, S. (1978) Computed crystal structure images for high resolution electron microscopy: *Nature* **274**, 322–324.
- Page, R. and Wenk, H. R. (1979) Phyllosilicate alteration of plagioclase studied by transmission electron microscopy: *Geology* **7**, 393–397.
- Paulus, M., Dubon, A., and Etienne, J. (1975) Application of ion-thinning to the study of the structure of argillaceous rocks by transmission electron microscopy: *Clay Miner.* **10**, 417–426.
- Phakey, P. P., Curtis, C. D., and Oertel, G. (1972) Transmission electron microscopy of fine-grained phyllosilicates in ultra-thin rock sections: *Clays & Clay Minerals* **20**, 193–197.
- Reynolds, R. C., Jr. (1967) Interstratification of clay systems: calculation of the total one-dimensional diffraction function: *Amer. Mineral.* **52**, 661–672.
- Reynolds, R. C. and Hower, J. (1970) The nature of interlayering in mixed-layer illite-montmorillonites: *Clays & Clay Minerals* **18**, 25–36.
- Roberson, H. E. and Lahann, R. W. (1981) Smectite to illite conversion rates: effects of solution chemistry: *Clays & Clay Minerals* **29**, 129–135.
- Ruehlicke, G. and Kohler, E. E. (1981) A simplified procedure for determining layer charge by the N-alkylammonium method: *Clay Miner.* **16**, 305–307.
- Spence, J. C. H. (1981) *Experimental High-Resolution Electron Microscopy*: Clarendon Press, Oxford, 370 pp.
- Spinnler, G. E., Self, P. G., Iijima, S., and Buseck, P. R. (1984) Stacking disorder in clinocllore chlorite: *Amer. Mineral.* **69**, 252–263.
- Spurr, A. R. (1969) A low viscosity epoxy resin embedding medium for electron microscopy: *Ultrastructure Res.* **26**, 31–43.
- Środoń, J. (1980) Precise identification of illite/smectite interstratifications by X-ray powder diffraction: *Clays & Clay Minerals* **28**, 401–411.
- Środoń, J. (1981) X-ray identification of randomly interstratified illite/smectite in mixtures with discrete illite: *Clay Miner.* **16**, 297–304.
- Środoń, J. (1984) X-ray powder diffraction identification of illitic materials: *Clays & Clay Minerals* **32**, 337–349.
- Tchoubar, C., Rautureau, M., Clinard, C., and Ragot, J. P. (1973) Technique d'inclusion appliquée à l'étude des silicates lamellaires et fibreux: *J. Microscopie* **18**, 147–154.
- Tessier, D. and Pedro, G. (1982) Electron microscopy study of Na smectite fabric—role of layer charge, salt concentration and suction parameters: in *Proc. Int. Clay Conf., Bologna, Pavia, 1981*, H. van Olphen and F. Veniale, eds., Elsevier, Amsterdam, 165–176.
- van Olphen, H. and Fripiat, J. J. (1979) *Data Handbook for Clay Materials and Other Non-Metallic Minerals*: Pergamon Press, Oxford, 346 pp.
- Veblen, D. R. (1983) Microstructures and mixed layering in intergrown wonesite, chlorite, talc, biotite and kaolinite: *Amer. Mineral.* **68**, 566–580.
- Yoshida, T. (1973) Elementary layers in the interstratified clay minerals as revealed by electron microscopy: *Clays & Clay Minerals* **21**, 413–420.
- Yoshida, T. and Suito, E. (1972) Interstratified layer structure of the organo-montmorillonites as revealed by electron microscopy: *J. Appl. Crystallogr.* **5**, 119–124.

(Received 15 March 1985; accepted 10 December 1985; Ms. 1473)